

# Bond disorder and spinon heat transport in the $S = \frac{1}{2}$ Heisenberg spin chain compound $\text{Sr}_2\text{CuO}_3$ : from clean to dirty limits

A. Mohan<sup>1</sup>, N. Sekhar Beesetty<sup>2</sup>, N. Hlubek<sup>1</sup>, R. Saint-Martin<sup>2</sup>, A. Revcolevschi<sup>2</sup>, B. Büchner<sup>1,3</sup>, C. Hess<sup>1,3</sup>

<sup>1</sup>*Leibniz Institute for Solid State and Materials Research IFW Dresden, 01069 Dresden, Germany*

<sup>2</sup>*Laboratoire de Physico-Chimie des Solides, Université Paris-Sud, 91405 Orsay, Cedex, France*

<sup>3</sup>*Center for Transport and Devices, Technische Universität Dresden, 01069 Dresden, Germany*

(Dated: April 4, 2024)

We investigate the effect of disorder on the heat transport properties of the  $S = \frac{1}{2}$  Heisenberg chain compound  $\text{Sr}_2\text{CuO}_3$  upon chemically substituting Sr by increasing concentrations of Ca. As Ca occupies sites outside but near the Cu-O-Cu spin chains, bond disorder, i.e. a spatial variation of the exchange interaction  $J$ , is expected to be realized in these chains. We observe that the magnetic heat conductivity ( $\kappa_{\text{mag}}$ ) due to spinons propagating in the chains is gradually but strongly suppressed with increasing amount of Ca, where the doping dependence can be understood in terms of increased scattering of spinons due to Ca-induced disorder. This is also reflected in the spinon mean free path which can be separated in a doping independent but temperature dependent scattering length due to spinon-phonon scattering, and a temperature independent but doping dependent spinon-defect scattering length. The latter spans from very large ( $> 1300$  lattice spacings) to very short ( $\sim 12$  lattice spacings) and scales with the average distance between two neighboring Ca atoms. Thus, the Ca-induced disorder acts as an effective defect within the spin chain, and the doping scheme allows to cover the whole doping regime between the clean and the dirty limits. Interestingly, at maximum impurity level we observe, in Ca-doped  $\text{Sr}_2\text{CuO}_3$ , an almost linear increase of  $\kappa_{\text{mag}}$  at temperatures above 100 K which reflects the intrinsic low temperature behavior of heat transport in a Heisenberg spin chain. These findings are quite different from that observed for the Ca-doped double spin chain compound,  $\text{SrCuO}_2$ , where the effect of Ca seems to saturate already at intermediate doping levels.

## I. INTRODUCTION

Quasi-particle transport in quantum systems has been a long standing unsolved issue from the point of view of both theory and experiment [1–28]. Much of the current interest is driven by theoretical discoveries of anomalous transport properties in quantum integrable systems [10, 24]. Ballistic heat transport at finite temperatures in integrable spin models, like the  $S = \frac{1}{2}$  Heisenberg chain, is a remarkable result that has received a lot of theoretical and experimental attention. Due to the integrability of the  $S = \frac{1}{2}$  Heisenberg chain, the intrinsic spinon heat transport is predicted to be non-dissipative, causing the heat conductivity to diverge [7, 28]. Experimental evidence of exceptionally large spinon heat conductivity and mean free path in 1D spin chains of the highly pure cuprate materials  $\text{SrCuO}_2$  and  $\text{Sr}_2\text{CuO}_3$ , has further strengthened this claim [1, 2, 4–6]. Though in a real system ever present extrinsic scattering mechanisms involving phonons and defects render the system non-integrable, thereby limiting the heat conductivity to finite values.

The large spinon heat conductivity in these systems also gives us a chance to systematically investigate extrinsic scattering processes, involving phonons and disorder, that spinons undergo to relax the heat current. Experimental investigations on these compounds by doping impurities in a controlled fashion have shown that a quantitatively reasonable description of the temperature dependence of spinon mean free paths is possible by taking into account the scattering of magnetic excitations off phonons and impurities alone [1, 2, 5, 6, 17].

Such quantitative descriptions falling under the framework of a semi-classical linearized Boltzmann theory, in spite of being empirical in nature, are able to model experimental observations with remarkable accuracy, thus becoming a valuable input to the theory of quasiparticle heat transport. A microscopic and fully quantum mechanical understanding of the underlying scattering processes in quasi one-dimensional systems is incomplete though. There do exist theoretical studies on transport of spinons in  $S = \frac{1}{2}$  Heisenberg chains coupled to phonons and impurities, which support the experimental observation that scattering by impurities at very low temperatures and by phonons at higher temperatures are the processes that dictate the temperature and doping dependence of the spinon mean free path [11, 19, 21–23]. But the understanding is far from complete even in this respect. This calls for more systematic experimental studies on clean and disordered  $S = \frac{1}{2}$  systems to probe the effects of defects/impurities on the spinon transport in such systems. Experimental work on  $S = \frac{1}{2}$  Heisenberg chain compounds becomes especially crucial as they offer the unique possibility to analyze directly the effect of spinon-phonon scattering processes on heat transport in a quantum spin system since spinon-spinon scattering is expected to be ineffective in relaxing the heat current in these systems.

The double spin chain compound  $\text{SrCuO}_2$  and the single spin chain compound  $\text{Sr}_2\text{CuO}_3$ , are two of the best realizations of a  $S = \frac{1}{2}$  Heisenberg spin chain model, differing mainly in the structure of the spin chains [29–31]. The materials' heat transport parallel to the chains is known to consist of a large contribution from spinons

in addition to conventional phononic transport [1, 2, 4–6]. Earlier,  $\text{SrCuO}_2$  has been studied with regard to the effect of substituting Ca for Sr in small amounts [3, 32]. These studies resulted in the following observations. Firstly, an off-chain impurity like Ca causing bond disorder in the spin chains has strong effects on the magnetic heat transport in these chains and opens a gap in the spin excitation spectrum at low energies. Secondly, the effect of Ca, viz. a strong suppression of  $\kappa_{\text{mag}}$ , decreases upon increasing its concentration and seems to saturate at around 10% Ca. This saturation was proposed to be related with the disorder-induced long distance decay of the spin-spin correlation [3]. In the present work, we chose the single chain compound,  $\text{Sr}_2\text{CuO}_3$ , for our study mainly because it contains a single spin chain as opposed to the two weakly interacting spin chains realized in  $\text{SrCuO}_2$ . Thereby we are now probing the effect of bond disorder on spinon transport in a more simplified chain structure that is different from the double chain  $\text{CuO}_2$  network in  $\text{SrCuO}_2$ . We observe a gradual but significant suppression of the spinon heat conductivity ( $\kappa_{\text{mag}}$ ) with increasing amount of Ca content which extends up to the highest doping level of 50 %, and thus is fundamentally different from that observed for the double chain compound  $\text{SrCuO}_2$ . Thus, Ca, an off-chain impurity, results in a more subtle effect than in-chain impurities [6] thereby making it possible to probe a large doping regime up to very high doping levels.

From our analysis we find that Ca can be described as an effective defect situated within the chain limiting the mean free path which ranges from very large ( $> 1300$  lattice spacings in pure  $\text{Sr}_2\text{CuO}_3$ ) to very short ( $\sim 12$  lattice spacings) at the highest doping level. Interestingly, we also observe that at maximum concentrations of Ca (50 %), the heat conductivity parallel to the chains increases almost linearly at high temperatures above  $\sim 100$  K thereby reflecting the behavior of the intrinsic spinon heat conductivity of a  $S = \frac{1}{2}$  Heisenberg chain.

## II. EXPERIMENTAL

Single crystals  $(\text{Sr}_{1-x}\text{Ca}_x)_2\text{CuO}_3$  with  $x = 0, 0.01, 0.05, 0.1$  and  $0.5$  were grown using the travelling solvent floating zone method. The starting materials used for preparing polycrystalline  $\text{Sr}_2\text{CuO}_3$  were  $\text{SrCO}_3$ ,  $\text{CuO}$  and  $\text{CaCO}_3$ , each of 99.99% purity. Measurements of the thermal conductivity in the range of 7–300 K were performed with a standard four probe technique wherein the temperature gradient was determined using a differential Au/Fe-Chromel thermocouple [15]. For the transport measurements rectangular samples with typical dimensions of  $(3 \times 0.5 \times 0.5) \text{ mm}^3$  were cut from the crystals for each doping level with an abrasive slurry wire saw. The longest dimension was taken parallel to the measurement axis.

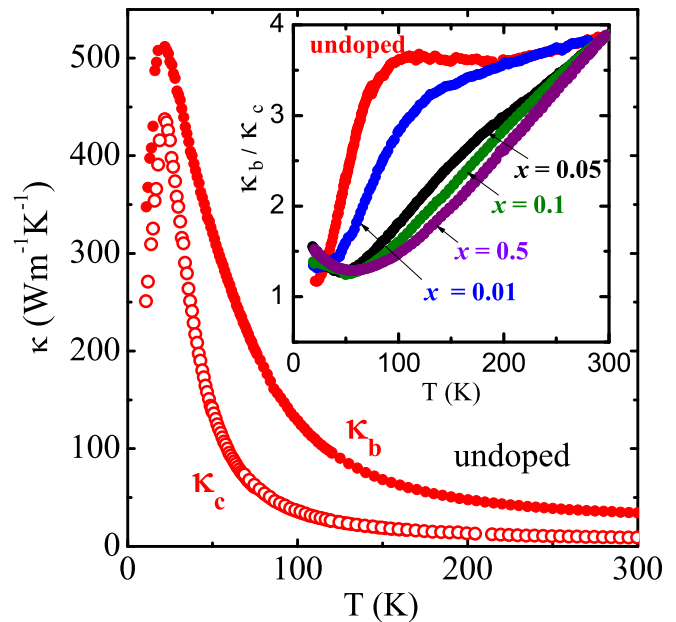


FIG. 1. (Color online) Heat conductivities  $\kappa_b$  measured parallel to the chains and  $\kappa_c$  measured perpendicular to the chains for the undoped  $\text{Sr}_2\text{CuO}_3$  compound, as a function of temperature (data from [5]). Inset: Ratio of heat conductivities  $\kappa_b$  and  $\kappa_c$  for  $\text{Sr}_2\text{CuO}_3$  and the doped compounds to give an idea of the magnitude and temperature dependence of the anisotropy in heat conduction. The curves for the doped compounds are normalized to the value of  $\kappa_b/\kappa_c$  for the pure compound at 300 K to illustrate the doping dependence of this ratio more clearly. The actual value of  $\kappa_b/\kappa_c$  at room temperature is always large ( $\sim 4$ ) and ranges from  $\sim 3.8$  for the pure compound to  $\sim 4.7$  for  $x = 0.5$ .

## III. RESULTS AND DISCUSSION

Fig. 1 recalls the heat conductivity measured parallel ( $\kappa_b$ : solid circles) and perpendicular ( $\kappa_c$ : open circles) to the spin chains of the undoped compound, as a function of temperature  $T$ . A large anisotropy in the measured heat conductivity is immediately obvious, with  $\kappa_b$  along the chains being much larger than  $\kappa_c$  perpendicular to the chains over the entire temperature range.  $\kappa_c(T)$  shows a sharp peak at low temperatures and falls off rather quickly at higher temperatures, a  $T$ -dependence characteristic of a purely phononic system. This heat conductivity perpendicular to the spin chains must be purely phononic because spinons possess dispersion only parallel to the chains.  $\kappa_b(T)$  shows a much broader peak at low  $T$  and falls off much slower than  $\kappa_c(T)$  at higher temperatures, untypical of phonon-only systems. The ratio of heat conductivities measured parallel ( $\kappa_b$ ) and perpendicular ( $\kappa_c$ ) to the spin chains of undoped  $\text{Sr}_2\text{CuO}_3$  is plotted as a function of temperature in the inset of Fig. 1), to give an idea of the magnitude of anisotropy and how it varies as a function of temperature and doping. Large anisotropy in the magnitude and temperature

dependence of  $\kappa_{\parallel}$  and  $\kappa_{\perp}$ , anisotropic dependence of heat conductivity on purity of compound, and unconventional temperature dependence of  $\kappa_{\parallel}$  have led to the well established conclusion that there is an additional contribution to the heat conduction parallel to the spin chains due to propagating magnetic excitations called spinons [1, 2, 4–6]. It is well confirmed that the difference between the two heat conductivities  $\kappa_{\parallel}$  and  $\kappa_{\perp}$  gives a good estimation of the spinon heat conduction in the system. This novel channel of heat conduction in these compounds exists in addition to the conventional channel of heat transport via phonons.

Fig. 2 shows the heat conductivity of the pure and doped compounds as a function of temperature, measured along the direction of the spin chains ( $\kappa_b(T)$ ). Upon doping, the broad peak in  $\kappa_b(T)$  at  $\sim 20$  K is reduced from  $\sim 512 \text{ W m}^{-1}\text{K}^{-1}$  at  $x = 0$  to  $\sim 350 \text{ W m}^{-1}\text{K}^{-1}$  at  $x = 0.01$ , and the shape of the curve changes. The broad peak in the undoped compound develops into a sharper phononic-like peak and a shoulder indicative of spinon contribution that has now reduced in magnitude. Increasing the Ca content to  $x = 0.05$  further suppresses the peak of  $\kappa_b$  to  $\sim 195 \text{ W m}^{-1}\text{K}^{-1}$ , and this trend continues up to  $x = 0.5$ . In the inset of Fig. 2, we see that for higher doping concentrations ( $x = 0.1$  and  $x = 0.5$ ) the heat conductivity shows a positive slope above  $\sim 100$  K up to 300 K. Whereas, for lower concentrations ( $x = 0.01$  and  $x = 0.05$ ) a negative slope exists up to 300 K, as in the case of the undoped compound.

Fig. 3 shows the heat conductivity measured perpendicular to the spin chains ( $\kappa_c(T)$ ). Upon doping increasing amounts of Ca, the peak magnitude of  $\kappa_c(T)$  gradually decreases as is expected for a purely phononic system due to increased scattering of phonons off Ca impurities. The black solid curves in Fig. 3 show fits for all Ca concentrations employing the Callaway model for phononic heat transport [33]. From Fig. 3 we see that the fits are good and the temperature dependence of the heat conductivity perpendicular to the spin chains is perfectly consistent with pure phononic heat transport. Decreasing magnitudes of  $\kappa_c$  with increasing concentrations of dopant can be captured in the model mainly by changing the parameter related to the phonon-defect scattering probability, thereby indicating enhanced scattering. Details regarding these fits are given in the appendix.

As can be inferred from the inset of Fig. 1 there is still a considerable anisotropy present in the heat conductivity of the Ca doped compounds signalling a still present and significant spinon contribution. It is well known that subtracting  $\kappa_c$  from  $\kappa_b$  provides a good estimate of the spinon heat conductivity ( $\kappa_{\text{mag}}(T)$ ) [1, 2, 4–6]. Fig. 4 shows  $\kappa_{\text{mag}}(T)$  for different doping levels of Ca. Here, we can see that  $\kappa_{\text{mag}}(T)$  drastically decreases for the Ca doped samples. Strong suppression of  $\kappa_{\text{mag}}$  indicates that in the doped compounds spinon transport is gradually impeded as a result of increasing scattering of spinons off defects induced by increasing amounts of Ca. For higher doping concentrations,  $x = 0.1$  and  $0.5$ ,

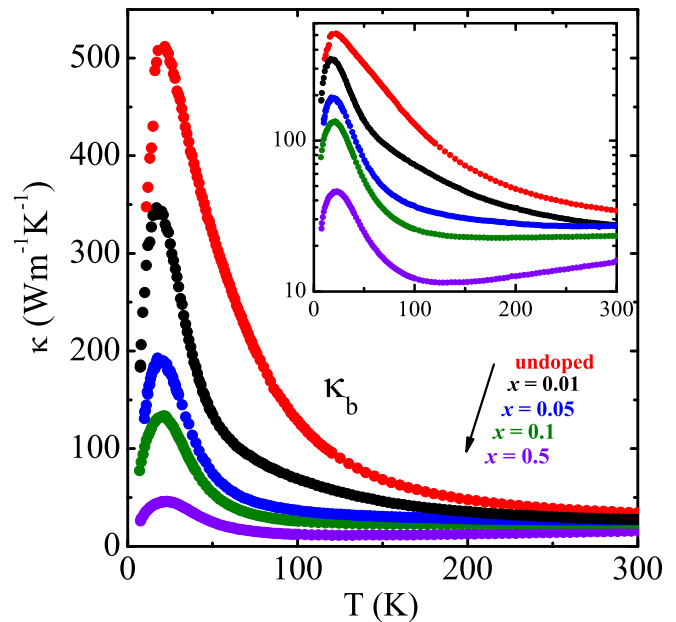


FIG. 2. (Color online) Heat conductivity  $\kappa_b$  as a function of temperature, measured parallel to the chains. Inset: A semi-log plot of  $\kappa_b$  versus temperature to better illustrate the changes upon introducing disorder.

we can clearly see that  $\kappa_{\text{mag}}$  increases at higher temperatures, with an almost linear increase for  $x = 0.1$ . This interesting observation reflects the intrinsic properties of spinon transport in a  $S = \frac{1}{2}$  Heisenberg spin chain as will be explained in more detail further below. The grey regions around the curves of  $x = 0.05$  and  $0.5$  doped Ca depict the uncertainty in  $\kappa_{\text{mag}}$  [34].

We now analyze  $\kappa_{\text{mag}}$  by extracting the mean free path of spinons,  $l_{\text{mag}}$ . It can be approached in two ways. One is by treating the low temperature spinon transport in the framework of a semi-classical kinetic model [1, 2, 4–6, 35], and the other is to use the more microscopic Drude weight approach [12, 13, 20, 25]. In theory, integrability of the spin-1/2 Heisenberg model results in a divergent  $\kappa_{\text{mag}}$  and is described by the product of the thermal Drude weight and a delta function at zero frequency. The low temperature behaviour of the Drude weight of a Heisenberg chain is linear in temperature and is given as [12, 13, 20, 25],

$$D_{\text{th}} = \frac{(\pi k_B)^2}{3\hbar} v T, \quad (1)$$

where  $v$  is the spinon velocity and  $k_B$  is the Boltzmann constant. Extrinsic scattering processes in a real system are expected to render the thermal conductivity of a single chain finite with a width  $\sim 1/\tau$ . [17] Thus, the magnetic heat conductivity for a single chain can be written as  $\tilde{\kappa}_{\text{mag}} = D_{\text{th}}\tau/\pi$ . Combining this with the expression for the Drude weight (Eq. 1) and using  $l_{\text{mag}} = \tau v$  we get a relation between the mean free path and the thermal conductivity of a real system,

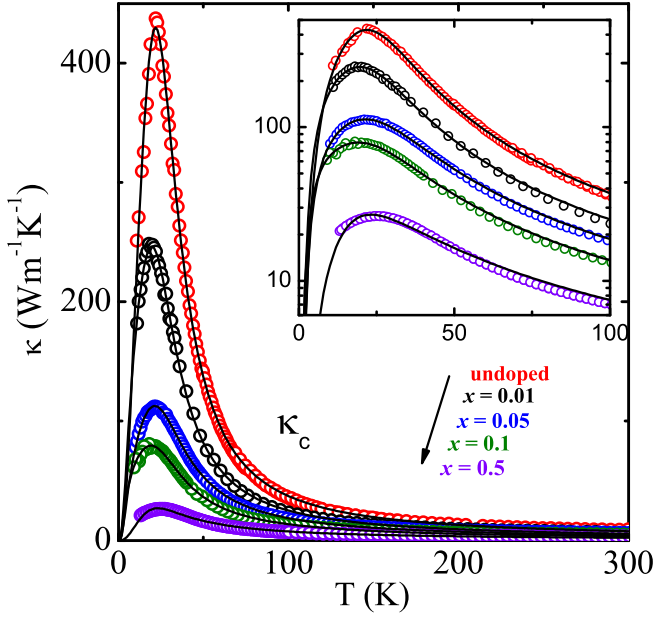


FIG. 3. (Color online) Heat conductivity  $\kappa_c$  as a function of temperature, measured perpendicular to the chains. Inset: A semi-log plot of  $\kappa_c$  versus temperature to better illustrate the changes upon introducing disorder. The solid black curves are fits to the curves according to the Callaway model.

$$l_{\text{mag}} = \frac{3\hbar}{\pi N_s k_B^2 T} \kappa_{\text{mag}}, \quad (2)$$

where  $N_s = 2/ab$  is the number of spin chains per unit area.

We mention that exactly the same expression can also be derived by starting with a simple kinetic model where  $\kappa_{\text{mag}} = \int C_k l_k v_k dk$ . Here  $C_k$  is the magnetic specific heat, and  $k$  denotes the momentum dependence [1, 2, 4–6, 35]. We now use Eq. 2 to extract and analyze the spinon mean free path.

$l_{\text{mag}}$  as a function of temperature for the pure and doped compounds is plotted in Fig. 5, the inset showing a semi-log plot of the same. Upon doping, the magnitude of the mean free path at low temperatures strongly and monotonically decreases, the trend being similar to that observed in  $\kappa_{\text{mag}}$ . In all cases,  $l_{\text{mag}}$  decreases with increasing  $T$ . Note that  $l_{\text{mag}}$  for  $x = 0.5$  is nearly constant at temperatures above 100 K, whereas for lower concentrations we see a temperature dependent decrease. As has been pointed out already for the pure compound [2, 5, 6], the  $T$ -dependent decrease can qualitatively be well explained by spinon-phonon scattering which becomes increasingly important with rising  $T$ . The doping-induced shortening of the mean free path can be qualitatively ascribed to strong spinon scattering due to Ca-induced disorder in the doped compounds. We model  $l_{\text{mag}}(T)$  using Matthiesen's rule and taking into account two scattering processes for spinons, viz. spinon-defect

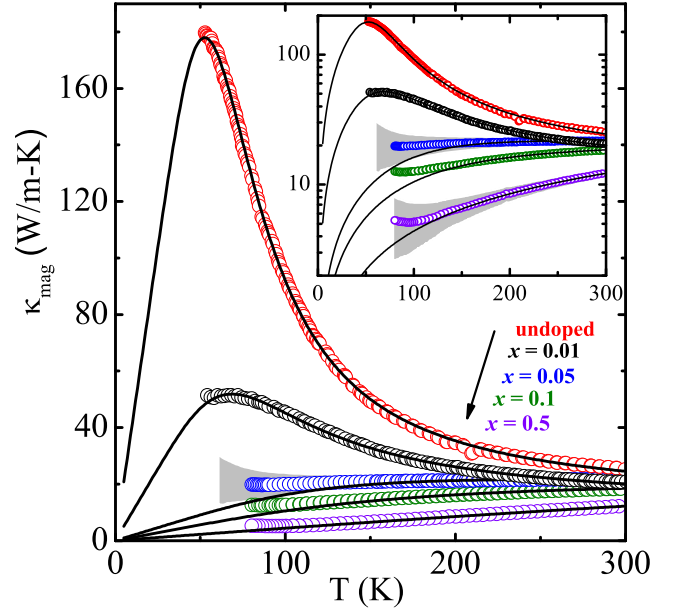


FIG. 4. (Color online) Magnetic heat conductivity  $\kappa_{\text{mag}}$  as a function of temperatures for the undoped and the Ca-doped compounds. Inset: A semi-log plot of  $\kappa_{\text{mag}}$  versus temperature to more clearly show the increase of  $\kappa_{\text{mag}}$  with increasing temperature for higher concentrations of Ca. Solid black lines are  $\kappa_{\text{mag}}$  recalculated using the fits for  $l_{\text{mag}}$  and Eq. 2. The grey regions depict the uncertainties associated with the extraction of  $\kappa_{\text{mag}}$ .

scattering and spinon-phonon scattering [1, 2, 4–6, 35]. Thus we have  $l_{\text{mag}}^{-1} = l_0^{-1} + l_{\text{sp}}^{-1}$ , where  $l_0$  describes the  $T$ -independent spinon-defect scattering whereas  $l_{\text{sp}}(T)$  accounts for the  $T$ -dependent spinon-phonon scattering. For the latter, we assume a general umklapp process with a characteristic energy scale  $k_B T_u^*$  of the order of the relevant phonon energies, which is commonly used in literature [1, 2, 4, 6, 35]. Thus we get the expression,

$$l_{\text{mag}}^{-1} = l_0^{-1} + \left( \frac{\exp(T_u^*/T)}{A_s T} \right)^{-1}, \quad (3)$$

which can be used to fit the data with  $l_0$ ,  $A_s$  and  $T_u^*$  ( $A_s$  is a measure of the coupling strength) as free parameters.

The fits for the undoped and doped compounds are shown in Fig. 5 and the fit parameters in Table I. We obtain good fits for the pure and  $x = 0.01$  compounds in the temperature range from 50–300 K, and for the  $x = 0.05, 0.1, 0.5$  compounds the fits are good in the temperature range from 150–300 K. It is apparently enough to take into account just spinon-defect scattering to describe the doping dependence of  $l_{\text{mag}}$  and umklapp-like spinon-phonon scattering to explain the  $T$ -dependence of  $l_{\text{mag}}$ , where the latter remains essentially the same upon doping. In order to fit the data, we have fixed  $T_u^*$  as 210 K (obtained by fitting  $l_{\text{mag}}$  for the pure compound) for the whole doping series allowing  $l_0$  and  $A_s$  to vary. In the model,  $T_u^*$  stems from the characteristic energy scale



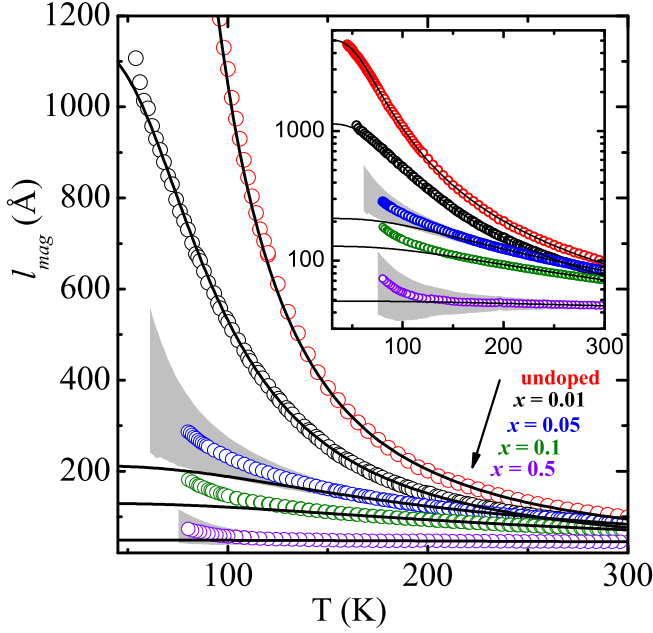


FIG. 5. (Color online) Mean free path of spinons as a function of temperature  $l_{\text{mag}}(T)$  and the fits according to Eq. 3. The grey region around the curve for 1 % Ca depicts the uncertainty associated with the calculation of  $l_{\text{mag}}$ . Inset: a semi-log plot of  $l_{\text{mag}}$  versus temperature.

$k_B T_u^*$  of the umklapp process, which is of the order of the Debye energy [1, 2] suggestive of acoustic phonons being involved in the scattering process. Hence, it is physically justified to fix  $T_u^*$  for the doped compounds, as the Debye energy is not expected to change substantially with doping.  $A_s$  changes slightly as a function of doping but is of the same order of magnitude for all doping levels. The slight variation in this parameter accounts for uncertainties in determining  $\kappa_{\text{mag}}$ , and a small variation in the spin-coupling strength in the pure and doped compounds.

The spinon-defect scattering length  $l_0$ , which represents a lower bound for the low- $T$  limit of  $l_{\text{mag}}$  and which should significantly depend on the sample's purity, decreases strongly upon doping and is very different for the pure and the doped compounds as can be seen in Table I. This parameter is most sensitive to changes in the Ca concentration, indicating that Ca defects primarily act as efficient barriers for the propagating spinons, i.e. the disorder-induced scattering can be well described by intra-chain defects. We mention that the deviation of the experimentally extracted  $l_{\text{mag}}$  from the fits at low temperatures ( $\lesssim 150$  K) can be attributed to the large error inherent in  $l_{\text{mag}}$  which is shown by the grey region surrounding the curves. As this error is large for the heavily doped compounds where the mean free paths are small, the fits are expected to be inaccurate at low temperatures.

Using the fits obtained for  $l_{\text{mag}}$ , we can recalculate

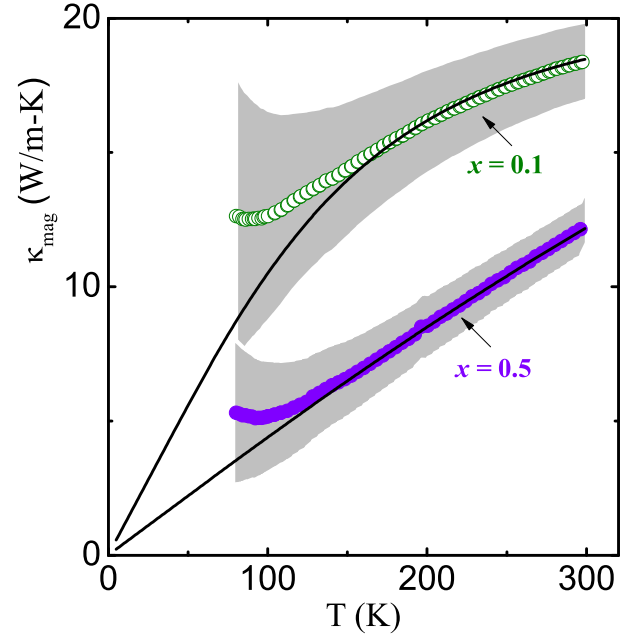


FIG. 6. (Color online) Magnetic heat conductivity  $\kappa_{\text{mag}}$  as a function of temperatures for the 10 % and 50 % Ca doped compounds. Solid lines are  $\kappa_{\text{mag}}$  recalculated using the fits for  $l_{\text{mag}}$  and Eq. 2. Grey regions around the curve indicate the uncertainties in  $\kappa_{\text{mag}}$ .

$\kappa_{\text{mag}}$  using Eq. 2, and plot these curves (black solid curves in Fig. 4) over the experimental curves to have a further illustration of the analysis. These recalculated curves, within the kinetic model, give us a good idea of the evolution of  $\kappa_{\text{mag}}$  in the entire temperature range, from the dilute doped compound, where it smoothly decreases with increasing temperatures, to the heavily doped compound where it increases almost linearly with increasing temperatures.

We now turn in more detail to  $\kappa_{\text{mag}}$  for the  $x = 0.1$  and  $x = 0.5$  doped compounds for which a monotonic increase with rising  $T$  is found (Fig. 6). Remarkably, an almost linear temperature dependence above  $T \approx 150$  K is seen for  $x = 0.5$ . Such a linear temperature dependence of  $\kappa_{\text{mag}}$  has been observed before in the highly disordered quasi one-dimensional compound  $\text{CaCu}_2\text{O}_3$  and reveals the intrinsic temperature dependence of the heat transport of a  $S = \frac{1}{2}$  Heisenberg chain [17]. It is well known

TABLE I. Fit parameters obtained by fitting  $l_{\text{mag}}$  by Eq. 3.

Ca content	$l_0$ (Å)	$T_u^*$ (K)	$A_s$ ( $10^5$ m/K)
0 %	5093	210	7.39
1 %	1139	210	8.19
5 %	212	210	4.85
10 %	127	210	4.2
50 %	48	210	1.19

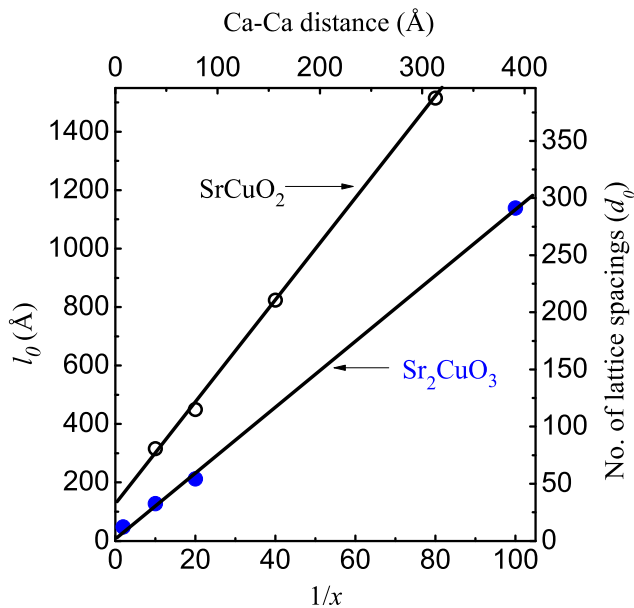


FIG. 7. (Color online) Spinon-defect scattering length,  $l_0$ , is plotted against the mean distance between two Ca atoms (lower x-axis) and the inverse of Ca concentration ( $x$ ) (upper x-axis) for SrCuO<sub>2</sub> (open symbols) and Sr<sub>2</sub>CuO<sub>3</sub> (filled symbols); the solid lines are linear fits to the data. The y-axis on the right gives an idea of the mean free path in terms of the number of lattice spacings between two Cu sites ( $d_0$ ).

that the temperature independent spinon-defect scattering mechanism that leads to a temperature independent  $l_{\text{mag}}$  is the dominant mechanism at low temperatures and at higher temperatures spinon-phonon scattering becomes dominant. Having large number of defects in the chain, which is the case for the doped compounds, will enhance the probability of spinons scattering off defects over that of spinons scattering off phonons. If the defect concentration is sufficiently high, the temperature dependence of the spinon-phonon scattering mechanism can be completely masked by the temperature independent spinon-defect scattering mechanism and, in turn, lead to a temperature independent spinon mean free path, i.e. a temperature independent scattering time  $\tau$ . Thus, the  $T$ -dependence of the experimental  $\kappa_{\text{mag}}$  represents directly that of the thermal Drude weight (Eq. 1).

Finally, in order to investigate the Ca-induced scattering process further, we plot the obtained values of the spinon-defect scattering length  $l_0$  as a function of the mean distance between two Ca atoms and the inverse of Ca concentration in Fig. 7. Here, we see that  $l_0$  scales perfectly with the inverse of Ca concentration as  $l_0 = 2.93(1/x)\text{\AA} \sim 3d_0$ , where  $d_0 = 3.91$  is the lattice spacing between two Cu sites along the chain [30, 31]. This corroborates that the Ca-induced bond disorder can perfectly be captured in terms of effective defects in the chain, where the scattering probability per defect is equally strong at all concentrations. From this plot we

also see that the Ca-Ca distance is smaller by a factor of 3 than the spinon-defect scattering length  $l_0$ .

We compare this finding with the results of a recent analogous study of the Ca-doped double spin chain compound, SrCuO<sub>2</sub> [3] (open symbols in Fig. 7). For this compound we see that  $l_0$  can be described as  $l_0 = 4.3(1/x)\text{\AA} + l_{\text{lim}}$ , where  $l_{\text{lim}}$  ( $\approx 140\text{\AA}$ ) is an offset. Therefore, the spinon-defect scattering length,  $l_0$ , does not scale with the inverse of the Ca concentration, indicating that already at intermediate concentrations ( $x = 0.1$ ) the effect of Ca saturates and the mean free path of spinons is not reduced any further upon increasing the Ca concentration. This is different from the perfect scaling that we observe for the single chain compound. The offset observed in Ca-doped SrCuO<sub>2</sub> was interpreted to be due to a limit set by the disorder-induced long distance decay of the spin-spin correlation ( $\xi$ ),  $\xi$  being calculated for a single  $S = \frac{1}{2}$  Heisenberg chain [3]. However, this claim does not seem to be valid in our case as the effect of Ca is equally strong at all doping levels. Thus, the proposed connection between the two quantities ought to be just a coincidence. We thus conclude that in the two compounds the difference in the effect of Ca-induced bond disorder could be in some way related to the difference in the chain structure. SrCuO<sub>2</sub> has a double chain structure with a finite interchain coupling as opposed to the single chain structure in Sr<sub>2</sub>CuO<sub>3</sub>. Although this coupling is small compared to the coupling strength within each chain, it seems to play an important role in deciding the effect of bond-disorder on the spinons propagating in these chains. This is evident as there is no other significant difference between these two compounds with regard to the spin system.

#### IV. CONCLUSION

We have studied the effect of introducing an off-chain impurity like Ca, thereby creating bond disorder, on the heat transport of the prototype single spin chain compound Sr<sub>2</sub>CuO<sub>3</sub>. We observe a drastic suppression of the magnetic heat conductivity parallel to the chains indicating that the propagation of spinons is very sensitive to even the slightest bond disorder. The temperature dependence of the mean free path of spinons can be modelled by spinon-defect and spinon-phonon scattering processes, and the reduction of the mean free path upon doping is accounted for mainly by increased scattering of spinons off effective in-chain defects, where the scattering probability per defect is equally strong in the entire doping range. This result is very different from the case of Ca-doped double spin chain compound SrCuO<sub>2</sub> where, presumably, finite inter-chain interaction reduces the effect of Ca at higher doping levels.

Interestingly, large disorder present in the compounds doped with high concentrations of Ca leads to a linearly increasing intrinsic spinon heat transport of the spin chain due to prevailing spinon-defect scattering and thus

a vanishing temperature dependence of the spinon mean free path. Thus, Ca-doped  $\text{Sr}_2\text{CuO}_3$  represents a unique case where the impact of impurities can be studied in a wide range of doping, covering very clean as well as very dirty limits.

## APPENDIX

TABLE II. Callaway fit parameters for the  $\kappa_c(T)$  curves.

Ca content	B ( $10^{-31} \text{ K}^{-1} \text{ s}^2$ )	b ( $10^{-44} \text{ s}^3$ )	A ( $10^{-4} \text{ m}$ )	L ( $10^{-4} \text{ m}$ )	$\Theta_D$ (K)
0 %	3.55	2.41	0.31	2.98	261 K
1 %	5.07	2.80	1.42	7.82	265 K
5 %	6.13	2.84	3.69	4.72	262 K
10 %	8.35	3.13	9.77	10.7	262 K
50 %	8.60	4.36	13.82	0.17	265 K

We model the phononic heat conductivity perpendicular to the chains using a phenomenological model devised by Callaway [33] using,

$$\kappa_{\text{ph}} = \frac{k_B}{2\pi^2 v_{\text{ph}}} \left( \frac{k_B T}{\hbar} \right)^3 \int_0^{\Theta_D/T} \frac{x^4 e^x}{(e^x - 1)^2} \cdot \tau_c dx. \quad (4)$$

Here  $x = \hbar\omega/k_B T$ ,  $\omega$  is the phonon angular frequency,  $\Theta_D$  is the Debye temperature and  $v_{\text{ph}}$  is the phonon velocity.  $\tau_c$  is a combined scattering rate, which is assumed to be the sum of individual scattering rates,

$$\tau_c^{-1} = \tau_B^{-1} + \tau_D^{-1} + \tau_U^{-1}, \quad (5)$$

where  $\tau_B$  denotes boundary scattering,  $\tau_D$  point defect scattering and  $\tau_U$  Umklapp scattering. Including the expressions for each scattering process,  $\tau_c$  can then be written as

$$\tau_c^{-1} = \frac{v_{\text{ph}}}{L} + A\omega^4 + B\omega^2 T \exp\left(-\frac{\Theta_D}{bT}\right), \quad (6)$$

with fit parameters  $L$ ,  $A$ ,  $B$ ,  $b$ .  $A$  describes the concentration of point defects,  $L$  describes the boundary scattering,  $B$  and  $b$  are intra-phonon scattering parameters. Fig. 3 shows  $\kappa_c(T)$  for all Ca concentrations and the corresponding Callaway fits. The obtained values of the free parameters from the best fit are given in Table II.  $\kappa_c(T)$  for the pure compound was fit first, and then  $\kappa_c(T)$  for the doped compounds were tried to be fit by keeping all other parameters except  $A$  fixed, i.e. only varying the phonon-defect scattering strength. It was found that it is not possible to fit the  $\kappa_c(T)$  curves just by changing this parameter. To obtain good fits, the intra-phonon scattering parameters and the boundary scattering length also had to be varied. One can see that the parameter  $A$  steadily increases with increasing concentration of Ca defects indicating the increasing strength of phonon-defect scattering, which is mainly responsible for the reduction of  $\kappa_c(T)$  upon doping. The difference in boundary scattering parameters only indicates a difference in the sample geometries. Finally, a small variation in parameter  $B$  could imply that the dopant possibly induces slight changes in the phononic dispersion branches, thereby affecting the scattering strength between phonons, in addition to playing the role of defects-like scatterers.

## ACKNOWLEDGMENTS

This work has been supported by the European Commission through the LOTHERM project (Project No. PITN-GA-2009-238475, and by Deutsche Forschungsgemeinschaft (DFG) through FOR912 (HE3439/8) and through the D-A-CH project HE 3439/12.

- 
- [1] A. V. Sologubenko, E. Felder, K. Giannò, H. R. Ott, A. Vietkine, and A. Revcolevschi, *Phys. Rev. B* **62**, R6108 (2000).
  - [2] A. V. Sologubenko, K. Giannò, H. R. Ott, A. Vietkine, and A. Revcolevschi, *Phys. Rev. B* **64**, 054412 (2001).
  - [3] N. Hlubek, P. Ribeiro, R. Saint-Martin, S. Nishimoto, A. Revcolevschi, S.-L. Drechsler, G. Behr, J. Trinkauf, J. E. Hamann-Borrero, J. Geck, B. Büchner, and C. Hess, *Phys. Rev. B* **84**, 214419 (2011).
  - [4] N. Hlubek, P. Ribeiro, R. Saint-Martin, A. Revcolevschi, G. Roth, G. Behr, B. Büchner, and C. Hess, *Phys. Rev. B* **81**, 020405 (2010).
  - [5] N. Hlubek, X. Zotos, S. Singh, R. Saint-Martin, A. Revcolevschi, B. Bchner, and C. Hess, *Journal of Statistical Mechanics: Theory and Experiment* **2012**, P03006 (2012).
  - [6] T. Kawamata, N. Takahashi, T. Adachi, T. Noji, K. Kudo, N. Kobayashi, and Y. Koike, *Journal of the Physical Society of Japan* **77**, 034607 (2008).
  - [7] X. Zotos, *Phys. Rev. Lett.* **82**, 1764 (1999).
  - [8] J. V. Alvarez and C. Gros, *Phys. Rev. Lett.* **89**, 156603 (2002).
  - [9] M. Azuma, M. Takano, and R. S. Eccleston, *Journal of the Physical Society of Japan* **67**, 740 (1998).
  - [10] H. Castella, X. Zotos, and P. Prelovšek, *Phys. Rev. Lett.* **74**, 972 (1995).
  - [11] A. L. Chernyshev and A. V. Rozhkov, *Phys. Rev. B* **72**, 104423 (2005).
  - [12] F. Heidrich-Meisner, A. Honecker, D. C. Cabra, and W. Brenig, *Phys. Rev. B* **68**, 134436 (2003).
  - [13] F. Heidrich-Meisner, A. Honecker, D. C. Cabra, and W. Brenig, *Phys. Rev. B* **66**, 140406 (2002).

- [14] C. Hess, B. Büchner, U. Ammerahl, L. Colonescu, F. Heidrich-Meisner, W. Brenig, and A. Revcolevschi, *Phys. Rev. Lett.* **90**, 197002 (2003).
- [15] C. Hess, B. Büchner, U. Ammerahl, and A. Revcolevschi, *Phys. Rev. B* **68**, 184517 (2003).
- [16] C. Hess, C. Baumann, U. Ammerahl, B. Büchner, F. Heidrich-Meisner, W. Brenig, and A. Revcolevschi, *Phys. Rev. B* **64**, 184305 (2001).
- [17] C. Hess, H. ElHaes, A. Waske, B. Büchner, C. Sekar, G. Krabbes, F. Heidrich-Meisner, and W. Brenig, *Phys. Rev. Lett.* **98**, 027201 (2007).
- [18] C. Hess, P. Ribeiro, B. Büchner, H. ElHaes, G. Roth, U. Ammerahl, and A. Revcolevschi, *Phys. Rev. B* **73**, 104407 (2006).
- [19] K. Louis, P. Prelovšek, and X. Zotos, *Phys. Rev. B* **74**, 235118 (2006).
- [20] A. Klümper and K. Sakai, *Journal of Physics A: Mathematical and General* **35**, 2173 (2002).
- [21] E. Orignac, R. Chitra, and R. Citro, *Phys. Rev. B* **67**, 134426 (2003).
- [22] A. V. Rozhkov and A. L. Chernyshev, *Phys. Rev. Lett.* **94**, 087201 (2005).
- [23] K. Saito, *Phys. Rev. B* **67**, 064410 (2003).
- [24] K. Saito, S. Takesue, and S. Miyashita, *Phys. Rev. E* **54**, 2404 (1996).
- [25] K. Sakai and A. Klümper, *Journal of Physics A: Mathematical and General* **36**, 11617 (2003).
- [26] E. Shimshoni, N. Andrei, and A. Rosch, *Phys. Rev. B* **72**, 059903(E) (2005).
- [27] E. Shimshoni, N. Andrei, and A. Rosch, *Phys. Rev. B* **68**, 104401 (2003).
- [28] X. Zotos, F. Naef, and P. Prelovsek, *Phys. Rev. B* **55**, 11029 (1997).
- [29] N. Motoyama, H. Eisaki, and S. Uchida, *Phys. Rev. Lett.* **76**, 3212 (1996).
- [30] C. L. Teske and H. Müller-Buschbaum, *Z. anorg. allg. Chem.* **379**, 234 (1970).
- [31] C. L. Teske and H. Müller-Buschbaum, *Z. anorg. allg. Chem.* **371**, 325 (1969).
- [32] F. Hammerath, S. Nishimoto, H.-J. Grafe, A. U. B. Wolter, V. Kataev, P. Ribeiro, C. Hess, S.-L. Drechsler, and B. Büchner, *Phys. Rev. Lett.* **107**, 017203 (2011).
- [33] J. Callaway, *Phys. Rev.* **113**, 1046 (1959).
- [34] As the method for extraction of magnetic heat conductivity relies on the assumption of isotropic phononic heat conduction, there could always be an error in our estimation that stems from the anisotropy of phononic conduction parallel and perpendicular to the chains. This error is large at low temperatures as the magnitudes of  $\kappa_b$  and  $\kappa_c$  are large in this regime, thus creating significant uncertainty in the extracted  $\kappa_{\text{mag}}$ . The errors have been calculated by taking into account a 30% anisotropy in the phononic heat conductivity parallel and perpendicular to the chains.
- [35] C. Hess, *The European Physical Journal Special Topics* **151**, 73 (2007).